JOURNAL OF MATERIALS SCIENCE **37** (2002) 3515–3520

Application of Taguchi method and orthogonal arrays for characterization of corrosion rate of IrO_2–RuO_2 film

KYUNG-SUN CHAE, HYEONG-KI CHOI
Biotechnology and Environmental Engineering Division, Agency for Technology and Standards, Kwacheon 427-010, Korea

JOON-HONG AHN, YO-SEUNG SONG
Department of Materials Engineering, Hankuk Aviation University, Koyang 412-791, Korea

DEUK YONG LEE*
Department of Materials Engineering, Daelim College of Technology, Anyang 431-715, Korea
E-mail: dylee@daelim.ac.kr.

$Ti/TiO_2/IrO_2$–RuO_2 electrodes were evaluated with an aid of Taguchi method and orthogonal arrays to elucidate the effect of the experimental parameters, such as type of intermediate layer between Ti substrate and IrO_2–RuO_2 film, heat treatment temperature, heat treatment time, and flow rate of air, on the corrosion resistance of the electrodes. Although the chemical composition of the as-deposited IrO_2–RuO_2 films was almost identical regardless of the processing conditions, it was found that the presence and the type of the TiO_2 intermediate layer was a critical factor to the anticorrosion properties of the $Ti/TiO_2/IrO_2$–RuO_2 electrodes among four different experimental parameters investigated. The optimal condition was the dip-coated IrO_2–RuO_2 film having the TiO_2 intermediate layer prepared by plasma spray and subsequently heat treated for 120 min at 450°C with air flow rate of 3 sccm.

1. Introduction

It is well-known that lead zirconate titanate (PZT) ferroelectric thin films have been considered as the material of choice for microelectronic device applications such as high density dynamic random-access memory capacitors and nonvolatile memories [1–6]. Recently, the transition metal oxides having the tetragonal rutile crystal structure has been proposed as the buffer layer to avoid the interface-related fatigue degradation between PZT thin film and the metal electrode [1, 3, 4]. These transition metal oxides such as IrO_2 and RuO_2 possess versatile merit such as low bulk resistivity (30–100 $\mu\Omega$-cm), excellent thermal stability, and diffusion barrier properties, which are prerequisite for the conducting materials [1, 4].

The effectiveness of the transition metal oxides can be extended to the electrode coating film for anticorrosion applications such as cathodic protection and to the oxygen evolving electrodes for electroflotation [7, 8]. Typical example in the corrosion industry is the IrO_2–RuO_2 film on Ti electrodes used for underground pipelines and cables, gas tanks, structural fixtures, and ships, which are exposed to the severely corrosive environments [7]. For the anticorrosion efficiency of the IrO_2–RuO_2 film on Ti electrodes, TiO_2 intermediate layer was employed by either sputtering or plasma spray to suppress the discontinuous formation of electrically insulating oxide (TiO_2) on the Ti electrode surface. The IrO_2–RuO_2 film was dip-coated and then dried for 10 min at 130°C and then annealed for 10 min at temperatures from 400 to 500°C in air.

It has been noted that Taguchi method is a powerful tool to determine the optimal condition of experimental parameters so that the performance characteristic is robust against noise factors [9]. In addition, its efficiency in experimentation offers various advantages over the existing approaches. In the present study, electrical properties of IrO_2–RuO_2 film prepared by a dip-coating process were investigated via Taguchi method and orthogonal arrays to determine the optimal setting and the relationship of experimental variables. Experimentally, four parameters were considered as follows: (1) preparation method of intermediate layer between Ti substrate and IrO_2–RuO_2 film; (2) heat treatment temperature; (3) heat treatment time; and (4) flow rate of air. Each parameter was further subdivided into 3 levels. Then, $L_9(3^4)$ orthogonal arrays were evaluated to optimize the performance characteristics of the dip-coated IrO_2–RuO_2 film.

*Author to whom all correspondence should be addressed.

2. Experimental procedure

The titanium substrate having a dimension of $50 \times 50 \times 3$ mm was polished using a SiC grit of 220 and then surface treated in 6N HC1 for 1 h at 90°C and distilled water. The film precursor solution was prepared by dissolution of 10 mol% $IrCl_3 \cdot 3H_2O$: 90 mol% $RuCl_3 \cdot xH_2O$ in isopropanol. After dip-coating, the specimen was firstly dried for 10 min at 130°C and then annealed for 10 min at temperatures from 400 to 500°C under air atmosphere (less than 1% hydrocarbon). The flow rate of air was varied from 3 to 7 standard cubic centimeter per minute (sccm). This drying process was repeated successively up to five times. Finally, dip-coated IrO_2–RuO_2 film was obtained by heat treatment for 60 to 120 min at temperatures from 400 to 500°C with 3 to 7 sccm air flow rate. TiO_2 oxide was chosen as the intermediate layer between the IrO_2–RuO_2 top-coat and the Ti substrate to improve the conduction. The intermediate layer of 3 μm and 15 μm in thickness was prepared by sputtering and plasma spray, respectively, and the experimental parameters were summarized in Table I.

Four experimental parameters are chosen and $L_9(3^4)$ orthogonal arrays are constructed as listed in Table II [9]. In Table II, A, B, C, and D indicate type of intermediate layer, heat treatment temperature, flow rate of air, and heat treatment time, respectively. Each variable is further subdivided into 3 levels. A_1, A_2, and A_3 represent non-bonding layer, intermediate TiO_2 layer prepared by sputtering, and by plasma spray, respectively. B_1, B_2, and B_3 imply 400, 450, and 500°C. C_1, C_2, and C_3 denote 3, 5, and 7 sccm, respectively. Lastly, D_1, D_2, and D_3 express 60, 90, and 120 min, respectively. Current density of the IrO_2–RuO_2 films in Table I was related to signal to noise (S/N) ratio to determine the optimized experimental condition and to reveal the influence of adjustment parameters on corrosion resistance of the IrO_2–RuO_2 film.

TABLE I Experimental conditions of $L_9(3^4)$ orthogonal arrays

No.	A	B	C	D
1	A_1	B_1	C_1	D_1
2	A_1	B_2	C_2	D_2
3	A_1	B_3	C_3	D_3
4	A_2	B_1	C_2	D_3
5	A_2	B_2	C_3	D_1
6	A_2	B_3	C_1	D_2
7	A_3	B_1	C_3	D_2
8	A_3	B_2	C_1	D_3
9	A_3	B_3	C_2	D_1

TABLE II Plasma spray and sputtering experimental conditions

Process variable	Plasma spray	Sputtering
Primary argon gas flow rate	80 sccm	500 sccm
Secondary hydrogen gas flow rate	15 sccm	
Vacuum level		8×10^{-3} torr
Power supply level	70 A, 500 V	3 kW
Rotating speed of substrate		10 rpm
Gun-substrate spray distance	85 mm	
Powder feed rate	3 kg/h	
Gun nozzle diameter	5 mm	

Polarization cell is composed of one working electrode (insoluble anode) and two counter graphite electrodes located inside the cell [8]. One reference electrode (saturated calomel electrode, SCE) was positioned as close as possible to the working electrode. The electrochemical measurements were conducted in 3.5 wt% NaCl at 25°C and 1500 mV (SCE) with a sweep rate of 600 mV/sec according to ASTM G5-94. The potential was measured by a potentiostat in the range of the open-circuit potential to 1800 mV. The details of the potentiodynamic polarization experiment were described elsewhere [8].

X-ray diffraction (XRD, XRD-3000, Rich Seifert Co., Germany) was performed to identify the composition of the IrO_2–RuO_2 films. A scan speed of 0.05° 2θ/sec was used in the 2θ range of 20° to 80°. Microstructure of the IrO_2–RuO_2 film and the TiO_2 intermediate layer was investigated with transmission electron microscopy (TEM, FEM-2000FX II, Jeol, Japan). Also, the coatings were quantitatively characterized by scanning electron microscopy (SEM) and energy-dispersive X-ray spectroscopy (EDX).

3. Results and discussion

Experimental anticorrosion current density having the properties of larger better was converted to S/N ratio according to the equation of $S/N = -10 \times \log[1/n\Sigma(1/j^2)]$, where n and j are the degree of freedom and the current density, respectively. The S/N ratio is listed in Table III. The optimal experimental condition can be achieved when the S/N ratio becomes the largest among the experiments investigated, because it is known that Taguchi analysis may give better reliability and predict the optimal processing setting under various adjustment parameter conditions [9]. The average and the contribution rate (ratio) of individual levels were calculated based on the S/N ratio and shown in Table IV. The variation of the average values of levels increased as the experimental parameters were varied from D → B → C → A, indicating that the influence of experimental parameters on the corrosion resistance became pronounced in the order of D(0.0024) < B(0.0099) < C(0.015) < A(0.016). It suggested that the subdivided levels were directly related to the anticorrosion current density of the IrO_2–RuO_2 film, therefore, small deviation of the contribution rate having a higher value in Table IV was more susceptible to the large divergence of the current density. In the present study, the optimal test condition having the highest contribution rate of the levels (anticorrosion

TABLE III S/N ratios determined by Taguchi analysis

No.	A	B	C	D	S/N ratio
1	A_1	B_1	C_1	D_1	0.0478
2	A_1	B_2	C_2	D_2	0.0444
3	A_1	B_3	C_3	D_3	0.0497
4	A_2	B_1	C_2	D_3	0.0405
5	A_2	B_2	C_3	D_1	0.0604
6	A_2	B_3	C_1	D_2	0.0571
7	A_3	B_1	C_3	D_2	0.0630
8	A_3	B_2	C_1	D_3	0.0761
9	A_3	B_3	C_2	D_1	0.0509

TABLE IV Average and contribution rate of individual levels

Individual level	Average	Contribution rate
A1	0.0473	-7.1×10^{-3}
A2	0.0537	-0.7×10^{-3}
A3	0.0633	8.9×10^{-3}
B1	0.0504	-4.0×10^{-3}
B2	0.0603	5.9×10^{-3}
B3	0.0525	-1.9×10^{-3}
C1	0.0603	5.9×10^{-3}
C2	0.0453	-9.1×10^{-3}
C3	0.0576	3.3×10^{-3}
D1	0.0530	-1.4×10^{-3}
D2	0.0554	1.0×10^{-3}
D3	0.0548	0.4×10^{-3}

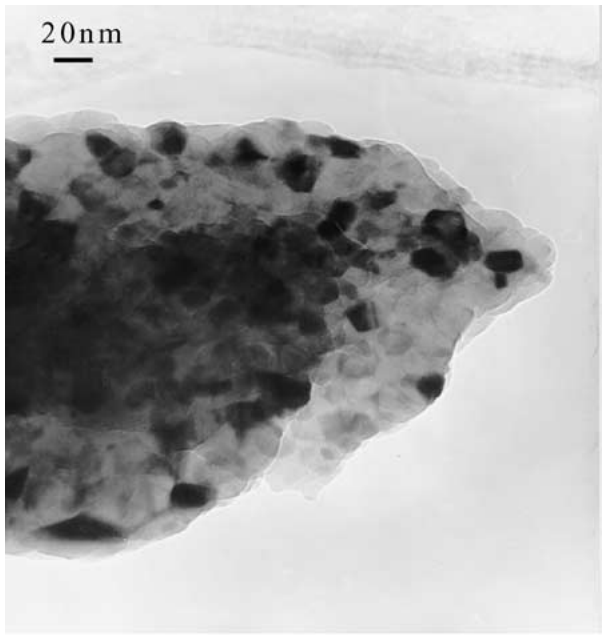

(a)

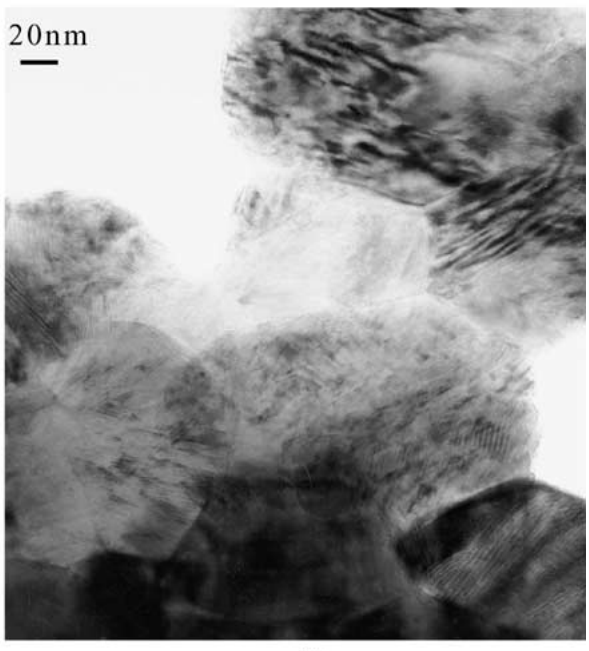

(b)

Figure 1 TEM image of TiO_2 layer prepared by (a) sputtering and (b) plasma spray.

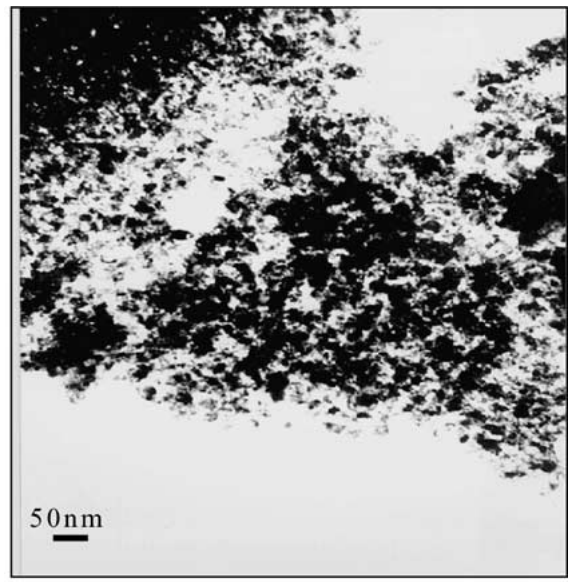

(a)

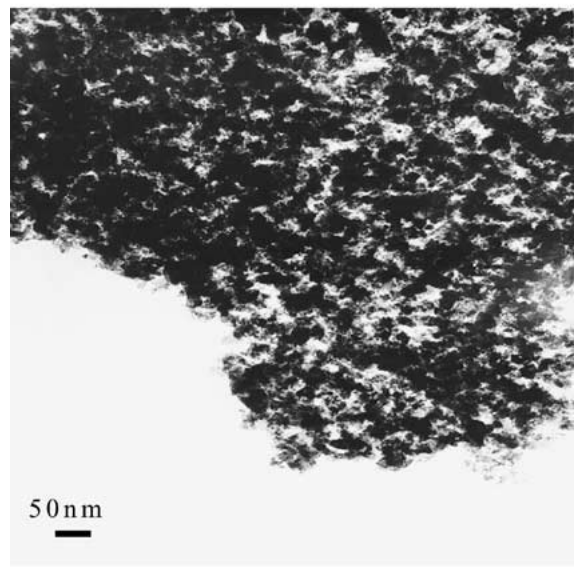

(b)

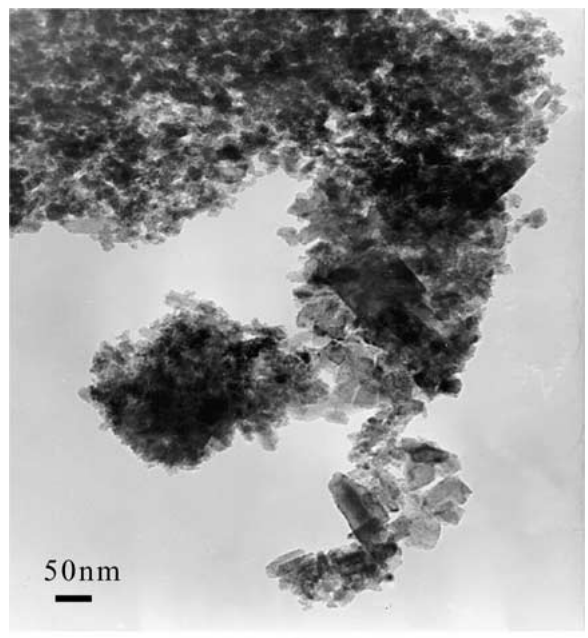

(c)

Figure 2 TEM image of IrO_2—RuO_2 film with various air flow rate of (a) 3 sccm, (b) 5 sccm, and (c) 7 sccm.

current density) was $A_3B_2C_1D_3$ as listed in Table III. Thus, the dip-coated IrO_2–RuO_2 film having the TiO_2 intermediate layer prepared by plasma spray (A_3) and subsequently heat treated for 120 min (D_3) at 450°C (B_2) with 3 sccm air flow rate (C_1) was likely to be the optimal experimental condition ($A_3B_2C_1D_3$).

For the comparison between the extremes in the present study, experimental current density of the sample no. 4 ($A_2B_1C_2D_3$) and no. 8 ($A_3B_2C_1D_3$) in Table I was examined by the potentiodynamic polarization test. Current densities of $A_2B_1C_2D_3$ and $A_3B_2C_1D_3$ at 1500 mV (SCE) are 0.040 A/cm^2 and 0.076 A/cm^2, respectively, showing that the current density of no. 8 (>0.05 A/cm^2) is effective to the corrosion resistance [8]. Fig. 1 is a TEM image of the TiO_2 intermediate layer, which demonstrates that the TiO_2 is composed of small grains. The shape and size of the TiO_2 grains ranged broadly from distorted spheres with diameters of 10–50 nm (sputtering, $A_2B_1C_2D_3$) and platelets with diameters of 180–240 nm (plasma spray, $A_3B_2C_1D_3$), respectively. Smaller grain size led to larger grain boundaries, which may act as a barrier to the current flow [7]. The conduction electrons are likely to be scattered by grain boundaries, resulting in the loss of current density. Lager grains ($A_3B_2C_1D_3$) of the as-plasma sprayed TiO_2 layer was obtained because plasma spraying employed a gun that simultaneously melts and propels small droplets of ceramic oxides onto the surface to be coated. Twinning was observed for the TiO_2 layer prepared by the plasma spray. It may be due to the plasma stream temperature that melts did not have enough mobility to relieve the stress generated by spray damage, resulting in deformation by twinning. Therefore, the difference in current density may be attributed to the disparity of microstructure caused by the different preparation method of the intermediate layer.

The effect of grain size on current density of Ti/IrO_2–RuO_2 electrodes was further investigated by changing the air flow rate (C) from 3 to 7 sccm. Grain size less than 10 nm was observed for the film prepared at the air flow rate of 3 sccm as shown in Fig. 2. Grain size increased from 20–40 nm to 15–80 nm and morphologies was changed from distorted spherical grain to elongated grain as the air flow rate rose from 5 to 7 sccm. As the grain size increased, the current density started to rise and then decreased. This result is in conflict with the former result, therefore, it is believed that the shape of the grains is more important than the grain size because the perimeter to diameter ratio increases

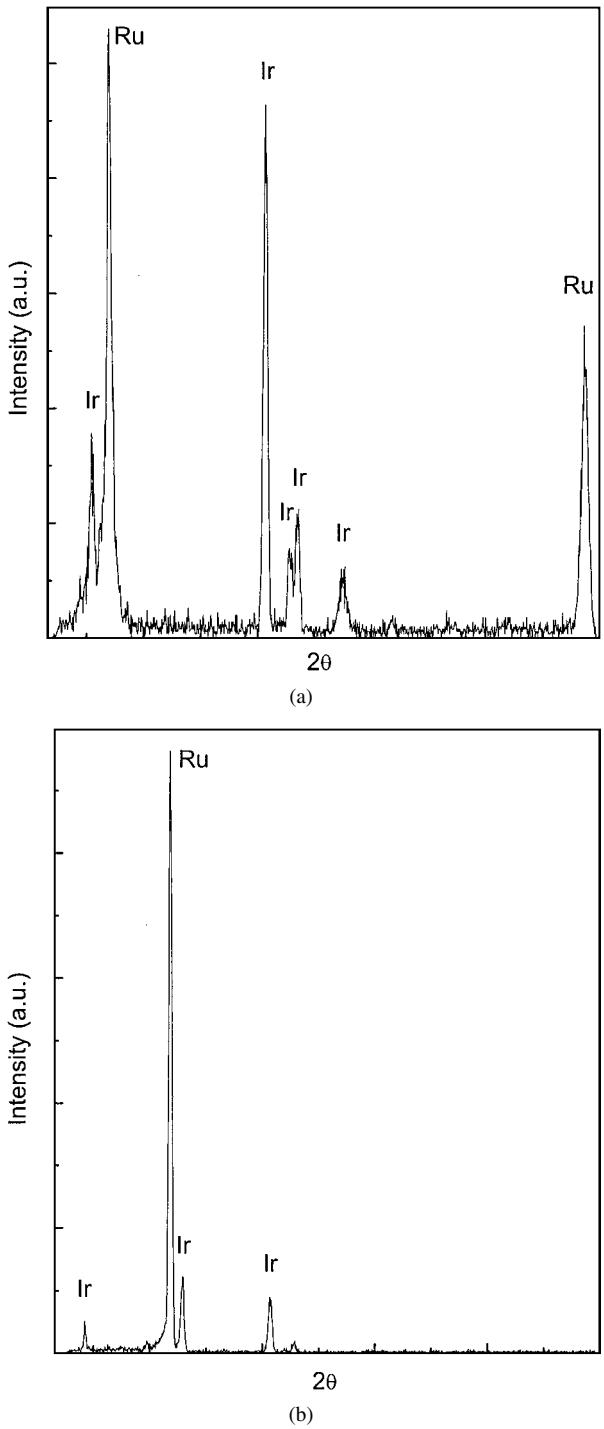

Figure 3 EDX analysis of (a) Ti/IrO_2–RuO_2 electrode at an air flow rate of 7 sccm; (b) Ti/TiO_2/IrO_2–RuO_2 electrode having the sputtered TiO_2 layer; (c) Ti/TiO_2/IrO_2–RuO_2 electrode having the plasma sprayed TiO_2 layer. (*Continued.*)

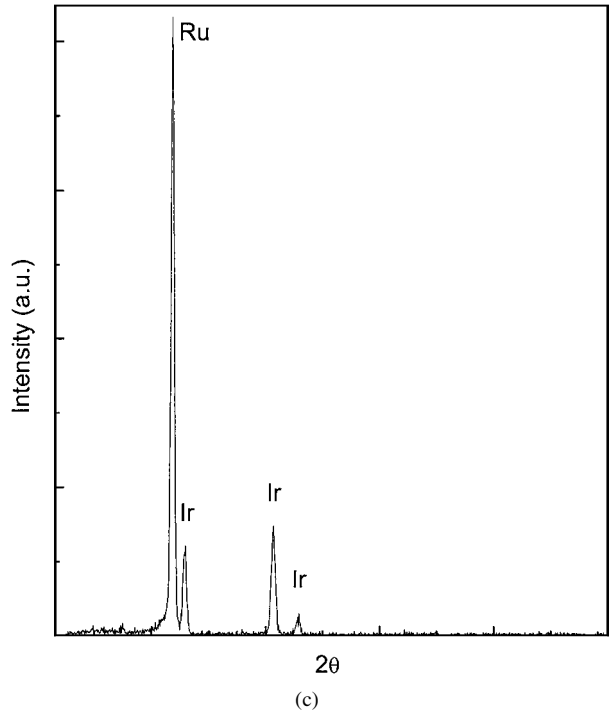

Figure 3 (*Continued.*)

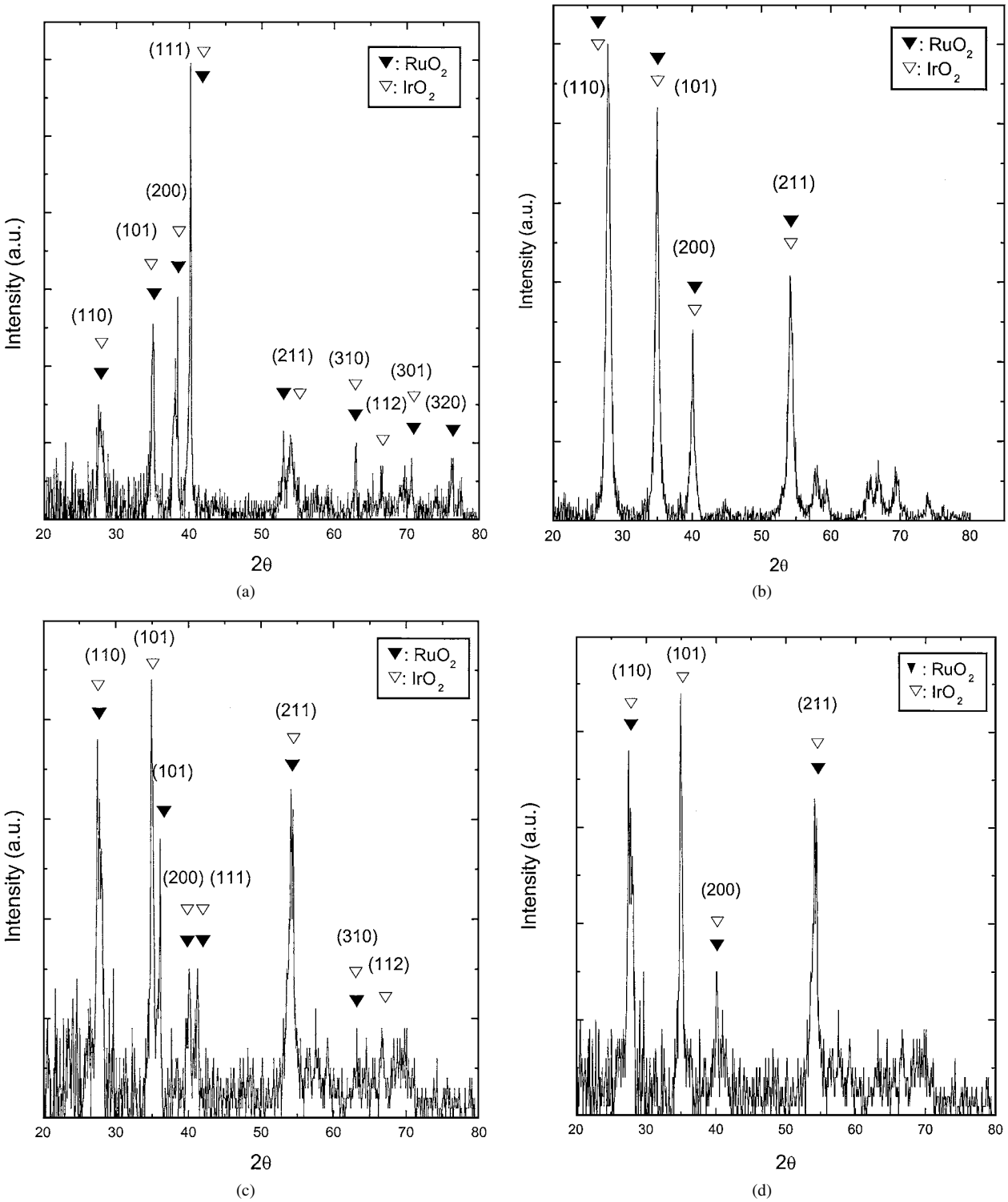

Figure 4 XRD patterns of specimen (a) no. 4 and (b) no. 8.

and then electron mean free path increases with fewer grain boundaries as a result of the grain morphology [5]. Therefore, it is noted that the contribution of *A* parameter to the anticorrosion behavior is more pronounced as compared to that of C parameter.

The composition of the IrO_2–RuO_2 top-coat film was examined quantitatively using SEM/EDX as shown in Fig. 3. Fig. 3a, b, and c represent the specimens without the TiO_2 buffer layer, with the sputtered TiO_2 layer, and the plasma sprayed TiO_2 layer, respectively. The composition of the as-deposited film, Ir : Ru = 9.53–11.76 wt% : 88.24–90.47 wt%, was maintained stoichiometric regardless of the type and the presence of the TiO_2 layer, indicating IrO_2/RuO_2 as the stable oxides [5]. The top-coat film was analyzed using XRD to identify the preferred orientation as shown in Fig. 4. Although the chemical composition of the as-deposited films was almost identical, the enhanced intensity of certain lattice planes ((110), (101), and (211)) in the film having the plasma sprayed TiO_2 layer (Fig. 4b–d) was not seen in the film having the sputtered TiO_2 layer (Fig. 4a) because the microstructure of the TiO_2 buffer layer may affect the growth behavior of the top-coat film [10], leading to the better anticorrosion properties of the electrode. It is conceivable in the present study that the corrosion resistance depends on the presence and the type of the TiO_2 intermediate layer, indicating that the as-deposited IrO_2–RuO_2 film

having the plasma-sprayed TiO_2 buffer layer may be highly effective.

4. Conclusions

The optimum process condition of the IrO_2–RuO_2 film on Ti electrodes for the corrosion resistance was evaluated by Taguchi method and orthogonal arrays and determined to be $A_3B_2C_1D_3$. Experimentally, the dip-coated IrO_2–RuO_2 film was composed of the TiO_2 intermediate layer prepared by plasma spray (A_3) and subsequently heat treated for 120 min (D_3) at 450°C (B_2) with 3 sccm flow rate of air (C_1). The current density of the resulting electrode was 0.076 A/cm^2, representing that it is effective to the corrosion resistance. It could be concluded that the presence and the type of the TiO_2 intermediate layer is dependent on the corrosion properties of the IrO_2–RuO_2 film on Ti electrode in this system.

References

1. L. KRUSIN-ELBAUM, M. WITTMER and D. S. YEE, *Appl. Phys. Lett.* **50**(26) (1987) 1879.
2. I. M. REANEY, K. BROOKS, R. KLISSURSKA, C. PAWLACZYK and N. SETTER, *J. Amer. Ceram. Soc.* **77**(5) (1994) 1209.
3. D. P. VIJAY and S. B. DESU, *J. Electrochem. Soc.* **140**(9) (1993) 2640.
4. L. KRUSIN-ELBAUM and M. WITTMER, *Ibid.* **135**(10) (1988) 2610.
5. L. KRUSIN-ELBAUM, *Thin Solid Films* **169** (1989) 17.
6. L. A. BURSILL and K. G. BROOKS, *J. Appl. Phys.* **75** (1994) 4501.
7. R. MRAZ and J. KRYSA, *J. Appl. Electrochem.* **24** (1994) 1262.
8. H. H. UHLIG and R. W. REVIE, "Corrosion and Corrosion Control" (John Wiley and Sons, Inc., New York, USA, 1985) p. 48.
9. K. DEHAND, "Quality Engineering in Production System" (McGraw-Hill, New York, 1989).
10. S. HORACEK and S. PUSCHAVER, *Chem. Eng. Prog.* **67** (1981) 71.

Received 26 April 2001
and accepted 9 April 2002